Touching the heart of HIV-1 drug resistance: the fingers close down on the dNTP at the polymerase active site

Stefan G Sarafianos[1], Kalyan Das[1], Jianping Ding[1], Paul L Boyer[2], Stephen H Hughes[2] and Edward Arnold[1]

Comparison of the recently solved structure of HIV-1 reverse transcriptase (RT)–DNA–dNTP ternary complex with the previously solved structure of RT–DNA binary complex suggests mechanisms by which the HIV-1 RT becomes resistant to nucleoside-analog inhibitors, drugs currently used in the treatment of AIDS.

Addresses: [1]Center for Advanced Biotechnology and Medicine (CABM) and Rutgers University Chemistry Department, 679 Hoes Lane, Piscataway, NJ 08854-5638, USA. [2]ABL-Basic Research Program, NCI-Frederick Cancer Research and Development Center, P.O. Box B, Frederick, MD 21702-1201, USA.

Correspondence: Edward Arnold
E-mail: arnold@cabm.rutgers.edu

Chemistry & Biology May 1999, **6**:R137–R146
http://biomednet.com/elecref/10745521006R0137

 ISSN 1074-5521

The numerous crystal structures of HIV-1 reverse transcriptase (RT) have significantly increased our understanding of DNA polymerization. Until quite recently all of the solved HIV-1 RT structures fell into one of three categories: unliganded [1–3]; in complex with a double-stranded DNA template–primer (dsDNA) and the Fab fragment of a monoclonal antibody (referred to as the RT–DNA binary complex) [4]; or in complex with non-nucleoside inhibitors (see [5] for review). HIV-1 RT is a dimer of two related subunits, a 66 kDa subunit (p66) and a 51 kDa subunit (p51) derived from the p66 subunit by proteolytic cleavage. The general shape of the polymerase domains of HIV-1 RT and other polymerases can be likened to a right hand with subdomains referred to as fingers, palm and thumb. In addition to the polymerase domain, the p66 subunit of HIV-1 RT contains an RNase H domain responsible for the hydrolytic cleavage of the RNA template in RNA–DNA duplexes. In the RT–DNA binary complex the primer terminus lies near three catalytically essential aspartic acid residues in the palm subdomain of p66; the DNA duplex extends along the enzyme surface toward the RNase H active site. The unliganded and DNA-bound structures represent snapshots of two of the early steps in polymerization. Although other polymerases have limited (or in the case of DNA polymerase β no known) homology to the HIV-1 RT, both the mechanism of polymerization and the structural changes involved are remarkably similar. A key structure of a ternary complex containing both nucleic acid and incoming dNTP has been described for polymerase β [6,7] and for type I DNA polymerases [8,9] but had not been solved for HIV-1 RT. Now the structure of the HIV-1 RT–DNA–dNTP complex has been solved and has provided valuable insight.

In a technological *tour de force*, the Harrison and Verdine laboratories [10] used a combination of clever chemical and biological engineering and careful crystallography to obtain a structure for an HIV-1 RT–DNA–dNTP ternary complex. Working with information from crystallographic studies of the RT in complex with DNA [4] and molecular-modeling studies [11] based on this binary structure, they chose residues in HIV-1 RT (Gln258, Gly262 and Trp266) that were close to the nucleic acid. Mutant RTs (Gln258→Cys, Gly262→Cys, Trp266→Cys) and modified dsDNA, which had a thiol group attached to the N2 position of a guanine base in the minor groove, were prepared (Figure 1). Huang *et al.* [10] hypothesized that, when close enough, the cysteine residue would become cross-linked to the modified nucleic acid. Single rounds of nucleotide addition were used to align the cysteine residues and the modified guanine (Figure 1). Based on this biochemical screening approach, the Gln258→Cys RT mutant was chosen for structural analysis. For crystallization, the modified RT was covalently cross-linked to a dsDNA that contained a modified guanine base in the template strand six base pairs from the polymerase active site. In addition to the Gln258→Cys mutation, other mutations were introduced into RT to facilitate purification and prevent oxidation without compromising the activity of the enzyme (Table 1).

Overall structure of the HIV-1 RT–DNA–dNTP ternary complex

Superposition of the structures of unliganded RT and the RT–DNA binary complex [2,3] showed that binding of the DNA involves a major conformational rotation of the thumb subdomain of p66. Comparison of the structures of the binary (RT–DNA) [12] and the ternary (RT–DNA–dNTP) [10] complexes suggests that the overall conformation of the DNA (excluding the single-stranded 5′-template overhang) is maintained after a dNTP enters the polymerase active site. The DNA is predominantly in the B form. The base pairs close to the polymerase active site have an A-like structure with a widened minor groove, which is also the case for DNA bound to other DNA polymerases [4,7–9,13–16]. In the binary complex the direction of the helical axis of the nucleic-acid substrate suggested that a longer template might pass through the crevice between the thumb and fingers [4,17]. In the ternary complexes of

Figure 1

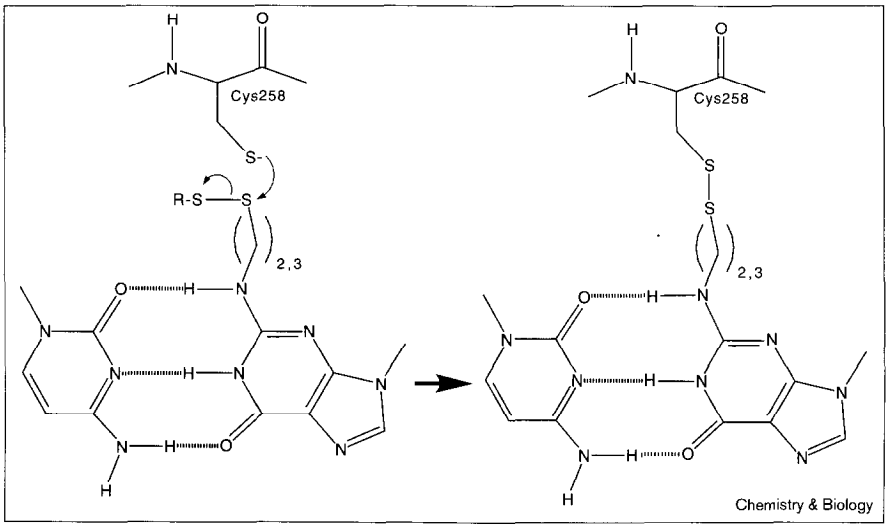

Chemistry of the cross-linking between the sidechain of engineered Cys258 of HIV-1 RT and a thiol group in the minor groove of DNA, which is attached by a trimethylene linker to the N2 position of a guanine base in the template strand.

HIV-1 RT and other polymerases the 5′ overhang of the template is bent away from the helical axis of the DNA duplex and extends over the outside surface of the fingers subdomain [6,8–10,16] (Figure 2).

Structure of the dNTP-binding site

Comparison of the structures of the ternary (RT–DNA–dNTP) and binary (RT–DNA) complexes reveals that binding of a dNTP induces substantial conformational changes in the HIV-1 RT [10]. Parts of the fingers subdomain rotate inwards towards the template–primer, bringing the tips of the fingers towards the palm sub domain and the polymerase active site (Figure 2). As a result of this movement, Lys65 and Arg72, conserved residues in the fingers subdomain, make contact with the incoming dNTP. Specifically, the ε-amino group of Lys65 and the guanidinium of Arg72 make salt bridges with the γ- and α-phosphates, respectively. Although this is the first report of the structural changes that take place when a dNTP binds to HIV-1 RT, similar structural changes in the fingers have been reported for other polymerases. In human DNA polymerase β, an enzyme with structural similarity but no evolutionary relationship to the HIV-1 RT, binding of a dNTP leads to a closing down of the subdomain equivalent to the fingers subdomain in RT [6]. In bacterial type I polymerases, enzymes distantly related to RT, the functional equivalent of a portion of the RT fingers subdomain has been shown to shift significantly towards the template–primer and the polymerase active site after binding of template–primer and dNTP

Table 1

Engineered mutations in HIV-1 RT.

Mutation/change	Function/role	Location
Gln258→Cys	Introduces cross-linking site	p66 thumb
Cys280→Ser	Prevents oxidative complications	p66 and p51 thumbs
Glu478→Gln	Eliminates RNase H activity	p66 RNase H
C terminus	His_6 tag facilitates purification	p51 C terminus

Figure 2

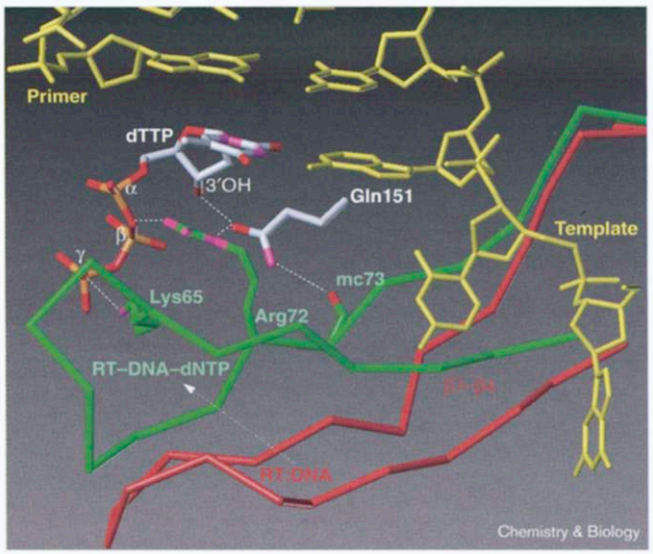

Open and closed conformations of dNTP-binding site of HIV-1 RT. The fingers in the binary complex (red) move towards the bound dNTP in the ternary complex (green). Lys65 and Arg72 interact with the γ- and α-phosphates of the dNTP, respectively. Gln151 is at the center of a hydrogen-bond network that involves the 3′-OH of dTTP, the mainchain carbonyl oxygen of Lys73 and the guanidinium of Arg72. Dashed lines indicate possible hydrogen bonds.

Figure 3

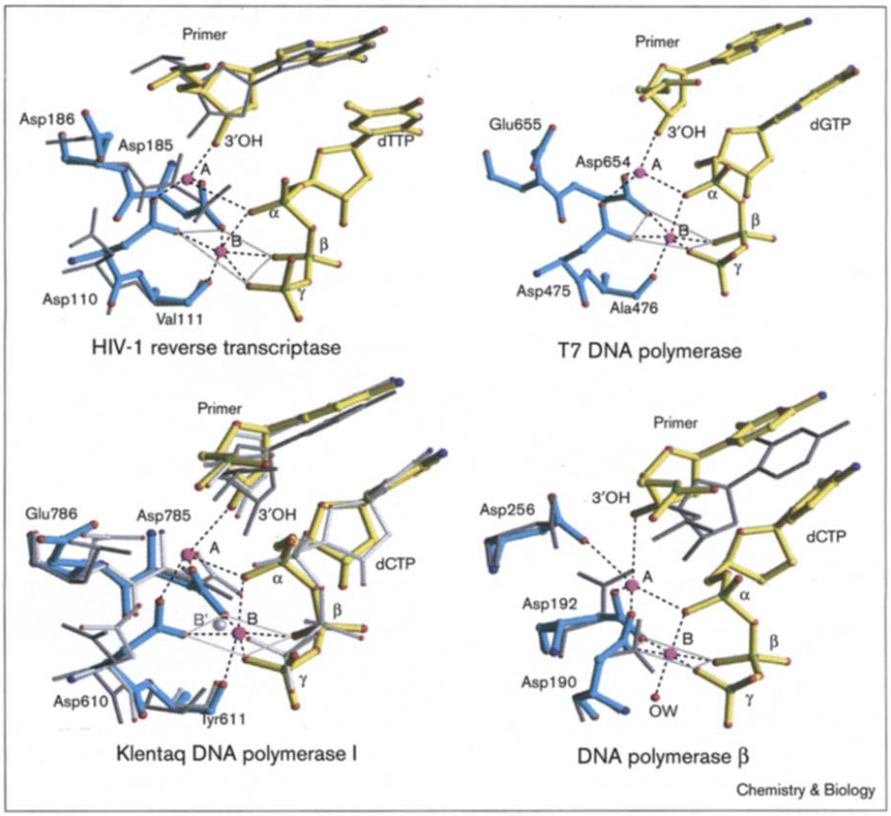

Metal chelation in polymerase active sites of four ternary enzyme (E)–DNA–dNTP complexes. The ternary complexes were superimposed on their corresponding binary (E–DNA) complexes (a binary complex structure is not available for the T7 DNA polymerase). In ternary complexes (E–DNA–dNTP) protein residues are cyan, metal ions are magenta and nucleotides are yellow. The only 'open' ternary complex, Klentaq–DNA–dCTP, is silver. Binary complex structures are gray. The octahedral coordination geometry of the nucleotide-binding metal ion B is highly conserved in all four polymerases. Axial positions are occupied by an α-phosphate oxygen and a mainchain carbonyl oxygen (in DNA polymerase β a water molecule coordinates the metal ion instead of a carbonyl oxygen). Equatorial positions are filled by two oxygens from β- and γ-phosphates and two δ-oxygens from two catalytic carboxylates. Catalytic metal ion A is ligated to the α-phosphate of dNTP, the 3′-OH of primer terminus and two oxygens from the carboxylates that chelate metal B. Although the first of the two chelating carboxylates maintains a similar orientation after binding of a dNTP, a sidechain rotation introduces the second chelating carboxylate (Asp110 in RT, Asp610 in Klentaq, Asp190 in polymerase β and possibly Asp475 in T7 polymerase) into coordinating position with metal ions A and B. A third carboxylate coordinates metal ion A only in polymerase β. Repositioning of the 3′-primer terminus is observed consistently after binding of dNTP. A 3′-OH was modeled on the primer 2′,3′ deoxyribose of the ternary complexes.

[8]. The Lys65–Arg72 pair of residues in RT is structurally analogous to the Arg518–Lys522 pair in T7 DNA polymerase [8], the Arg754–Arg758 pair in the Klenow fragment [18] and the Arg659–Lys663 pair in Klentaq [9], respectively. The structural analogy between these pairs is consistent, at least in the cases of HIV-1 RT and the Klenow fragment; biochemical experiments have suggested that Arg72 [19] and Lys65 of HIV-1 RT [20] and Arg754 and Arg758 of the Klenow fragment [21] are involved in pyrophosphate binding.

Binding of dNTP and metals consistently induces sidechain repositioning at polymerase active sites. In the structures of the binary (enzyme–DNA) or ternary (enzyme–DNA–dNTP) complexes that are available, similar changes are seen: there is a repositioning of the primer 3′ terminus with respect to the rest of the polymerase active site; and there is considerable rearrangement of the carboxylate sidechains that brings one carboxylate (Asp110 in HIV-1 RT, Asp610 in Klentaq or Asp192 in polymerase β) close enough to the metal ion brought in by the incoming dNTP to permit chelation (metal ion B; Figure 3).

Reminiscent of the metal coordination reported in previous high-resolution structures of ternary complexes of polymerases with DNA and ddNTPs [6,8], the two divalent metal ions in the RT–DNA–dNTP ternary complex coordinate the oxygens of all three phosphates of the dNTP, the sidechains of strictly conserved Asp185 and Asp110, as well as the backbone carbonyl oxygen of Val111. The metal ions are also close to the expected position of the primer 3′-OH, which is absent from the dideoxy-terminated DNA in the RT ternary structure. The two Mg^{2+}, one catalytic (A) and the other nucleotide-binding (B) [6], are believed to facilitate an SN_2 nucleophilic attack by the 3′-OH of the primer terminus on the α-phosphorus of the incoming dNTP and to stabilize the negative charge in the transition state [6,8,22]. In the ternary complexes the triphosphate is coordinated to the nucleotide-binding metal ion (B) as an α-, β-, γ-tridentate Mg^{2+}–dNTP complex [6,8]. The conformation of the triphosphate moiety is similar to that found in crystal structures of free Na^{+}–ATP and Mg^{2+}–dNTP in solution [6,23,24]. The similarity of Mg^{2+}–dNTP in solution and at the active site of polymerases may provide a significant entropic advantage for a reaction that has a fast turnover

Table 2

Residues in the dNTP-binding pocket of HIV-1 RT and functional homologs in Klenow fragment, T7 DNA polymerase and Klentaq.

Residue in RT (Klenow/T7 DNA pol/Klentaq)	Possible function	Comment
Interactions with dNTP phosphates		
Arg72 (Arg758/Lys522/Lys/663)	dNTP binding, PPi removal	Arg72→Ala RT and Arg758→Ala Klenow are deficient in pyrophosphorolysis; Arg72 guanidinium also stacks with base of dNTP
Lys65 (Arg754/Arg518/Arg659)	dNTP binding, PPi removal	Arg754→Ala Klenow is deficient in pyrophosphorolysis [21]
Interactions at 3′ pocket with sugar ring and base		
Gln151 (Phe762/Tyr526/Phe667)	Recognition of 3′-OH of dNTP and sugar ring	Mutants of RT and *Thermus aquaticus* polymerase have altered sensitivities to ddNTPs
Tyr115 (Glu710/Glu480/Glu615)		
Active-site carboxylates		
Asp110 (Asp705/Asp475/Asp610), Asp185 (Asp882/Asp654/Asp785), Asp186 (Glu883/Glu655/Glu786)	Metal-ion chelation, catalysis of bond formation	Asp186 and its homologs do not chelate metals in structures of ternary complexes
Interactions with primer terminus		
Met184 (His881/His653/His784)	Positioning of 3′-primer terminus, binding of dNTP	Crystal structure of Met184→Ile mutant shows shifted primer terminus [47]

rate. Although it has been proposed that the three conserved acidic residues are involved in metal-ion binding during polymerization by RT and other polymerases [25,26], only two carboxylate residues appear to be coordinated to metals in HIV-1 RT, T7 polymerase and Klentaq [8–10]. Nevertheless, mutation of any of the three carboxylates results in severe impairment in polymerization [25,27–29], underscoring the importance of all three groups in the reaction. A possible role for the third carboxylate (Asp186 in HIV-1 RT, Glu883 in the Klenow fragment and Glu655 in T7 DNA polymerase) might be to help position the primer terminus by interacting with an oxygen atom of the 3′-terminal phosphate [12]. In the T7 DNA polymerase, a third carboxylate (Glu655) has a similar indirect interaction with the 3′-terminal phosphate of the primer strand, mediated by a conserved and indispensable residue (His704) [8]. Other similarities in the dNTP-binding pocket of polymerases are based on steric and electrostatic constraints that are summarized in Table 2 and shown in Figure 4 for HIV-1 RT.

The rearrangement that takes place upon dNTP binding to HIV-1 RT creates what Huang *et al.* [10] have called the '3′ pocket'. This pocket accommodates the 3′-OH of the incoming dNTP and is lined with the sidechains of the conserved residues Ala114, Tyr115 and Gln151, as well as by the peptide backbone between Asp113 and Tyr115. Because the nucleoside analogs used as reverse-transcriptase inhibitors (NRTIs) all lack a 3′-OH, residues of the 3′ pocket play important roles in the HIV-1 RT becoming resistant to NRTIs, as will be discussed below. A similar interaction between the 3′-OH of the incoming dNTP and Tyr526 is seen in the ternary structure of T7 DNA polymerase [8] (Table 2); mutation of this residue alters the sensitivity of T7 DNA polymerase to ddNTPs [30], consistent with a role for Tyr526 in recognizing the 3′-OH of the incoming dNTP.

Although there is no reason to suspect that adenylyl cyclase is evolutionarily related to polymerases, the coordination geometry proposed for the binding of ATP to adenylyl cyclase is quite similar to the binding of dNTP by HIV-1 RT [31,32]. Both HIV-1 RT and adenylyl cyclase catalyze a phosphoryl-transfer reaction. Unlike DNA polymerases, which catalyze a bimolecular reaction, in the reaction catalyzed by adenylyl cyclase the 3′-OH of the ATP substrate is the nucleophile that attacks the α-phosphate of the same ATP molecule, converting it to cyclic 3′5′-AMP and releasing PP_i. In adenylyl cyclase, as in HIV-1 RT, two divalent metal ions are proposed to bind two carboxylates and a backbone carbonyl of the adenylyl cyclase V $C_{1\alpha}$ domain, as well as the three phosphates of ATP. The interactions of Arg72–Lys65 with the phosphates of dNTP in HIV-1 RT are similar to the interactions of Arg1029 of the α4 helix and Lys1065 of the β7–β8 loop of an adjacent adenylyl cyclase II C2 subunit. Upon ATP binding, the β7–β8 loop of adenylate cyclase undergoes a conformational change similar to the closing of the fingers subdomain of HIV-1 after binding a dNTP. The interactions within the active sites of divergent polymerases and adenylyl cyclase is consistent with a universal strategy for metal-assisted phosphoryl transfer by evolutionary unrelated enzymes.

Resistance to nucleoside reverse transcriptase inhibitors

Although the emergence of NRTI-resistant viruses has been a major problem in the treatment of AIDS, NRTIs

Figure 4

A view of the dNTP-binding pocket in the ternary RT–DNA–dNTP complex. The color code for Van der Waals volumes shown is as follows: residues at the 3′- pocket, green; residues involved in resistance to AZT, blue; residues interacting with template and primer, cyan. Potential interactions are shown as yellow dotted lines. For the sake of clarity some active-site residues have been omitted.

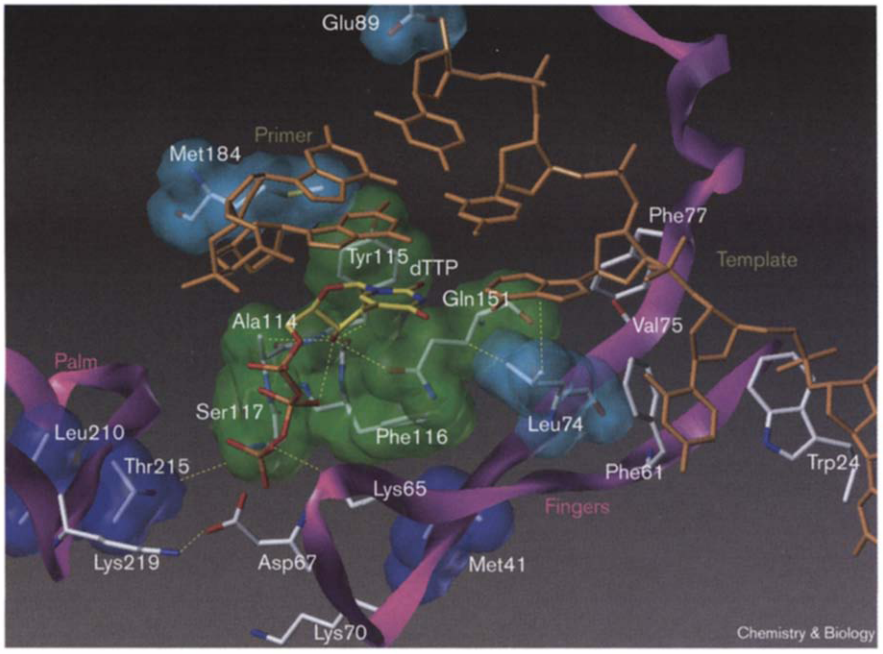

remain key components in current combination-drug therapies. Understanding the molecular aspects of NRTI resistance has been complicated by intricate patterns of mutations and resistance data that do not always correlate with the available biochemical and structural information. For example, most of the nucleoside-resistance mutations were not in the dNTP-binding site of the binary RT–DNA complex [4]. Molecular modeling based on the structure of the binary complex [17] suggested that most NRTI mutations were likely to alter the interactions of RT with the template–primer. We now know from the structure of RT–DNA–dNTP that the extended template overhang bends away from the DNA duplex [10] and most NRTI-resistance mutations are closer to the bound dNTP than previously predicted. Although repositioning of template–primer remains a mechanism for inducing resistance to NRTIs (Table 3), the new structure [10] suggests that NRTI resistance mutations can also affect inhibitor binding by directly changing interactions with inhibitor or by indirectly altering residues proximal to the dNTP-binding pocket. Some of the mutations listed in Table 3 are discussed below in view of these mechanisms.

In the crystal structure of the ternary complex, Gln151 interacts directly with the 3′-OH and the β phosphate of dNTP, as well as with residues that either directly interact with dNTP (e.g. Arg72, which hydrogen bonds with dNTP) or affect the position of important structural elements (e.g. the mainchain carbonyl oxygen of residue 73 hydrogen bonds with Gln151, bridging the palm and fingers subdomains) [10]. The Gln151→Met mutation might therefore engender multidrug resistance to AZT, d4T and ddC/ddI (NRTI drugs) [33,34] by inducing both direct and indirect changes at the dNTP-binding pocket. The Gln151→Met mutation is generally accompanied by mutations at four neighboring residues (Ala→62Val, Val75→Ile, Phe77→Leu and Phe116→Tyr; Table 3). These secondary mutations appear to 'fine tune' and reinforce the effects of the primary mutation both by increasing resistance and by improving polymerase activity, which is impaired by mutation at Gln151 [33,35].

In the structure of RT–DNA–dNTP, Leu74 is not in a position to directly affect dNTP binding. However, it does interact with the template nucleotide that is base paired to the incoming dNTP and is also proximal to Gln151, which is a key residue in the dNTP-binding pocket. The Leu74→Val mutation might therefore reduce sensitivity to ddI and ddC [36] by altering template position [10,17] and/or by affecting the orientation of the Arg72 and Gln151 sidechains [10]. The Lys65→Arg mutation is also associated with resistance to ddC, ddI [37,38] and PMEA [39]. The Lys65→Arg mutation probably affects the interaction of the RT with the triphosphate moiety of dNTPs, and might also alter the nucleotide-binding specificity of the enzyme.

A recently reported mutation that confers resistance to several nucleoside analogs is an insertion of two or more residues (usually serines) after position 69 in HIV-1 RT ([40] and references in [41]). This insertion is likely to indirectly affect the dNTP-binding pocket, and might affect the interactions of neighboring residues Lys65,

Table 3

HIV-1 RT residues involved in resistance to NRTIs.

Residue change	Resistance phenotype	Mechanism	Comments
Met41→Leu	AZT	Causes indirect rearrangement of dNTP-binding pocket through residue 116	Found with Thr215→Tyr/Phe, which might 'tune' its effect
Lys65→Arg	PMEA, ddC, ddI, 3TC	Packing rearrangement of dNTP through interactions with γ-phosphate of dNTP and Arg72	Suppresses resistance to AZT
Asp67→Asn	AZT	Changes interaction with residue 219 and formation of dNTP-binding pocket	Might 'tune' effects of Thr215→Tyr/Phe
69–Ser–Ser–X	AZT+d4T+ddI/ddC (MDR)	Possible conformational effect on fingers loop, transmitted to dNTP by contacts from other residues	Insertion can also be after Ser68 [68]
Lys70→Arg	AZT	Arg70 might make a new hydrogen bond with γ-phosphate of dNTP or Asp113	β3–β4 poorly ordered in Huang *et al.* [10]
Leu74→Val	DdI, ddC, DXG	Template repositioning; packing rearrangements of dNTP through interactions with Arg72 and Gln151	Suppresses resistance to AZT
Val75→Thr	DdC, d4T, d4C	Might modify hydrophobic core of fingers and interactions of residue 151 with dNTP. Template repositioning	mc75 interacts with template through hydrogen bond
Glu89→Gly	ddG	Template repositioning	Cross-resistant to foscarnet
Gln151→Met	AZT+d4T+ddI/ddC (MDR)	Key residue. Resistance might be caused by disruption of hydrogen-bond network involving Gln151, mainchain residue 73, 3′-OH of dNTP, γ-phosphate and Arg72	Associated with mutations at positions 62, 75, 77 and 116; causes MDR alone. Two-base mutation.
Met184→Ile/ Met184→Val/ Met184→Thr	3TC, (-)FTC, L-FddC	Steric interactions between sidechain of β-branched residue at position184 and ring of β-L-enantiomer of NRTI. Template–primer repositioning	Met184→Ile/Val restores AZT sensitivity to Thr215→Tyr/Phe AZT mutants
Leu210→Trp	AZT	Stabilize hydrophobic substitution at position 215	No effect alone
Thr215→Tyr/ Thr215→Phe	AZT	Hydrophobic substitution may reposition Asp113 and affect structure of 3′ pocket that accommodates azido group of AZT. Needs further hydrophobic stabilization provided by Met41→Leu and Leu210→Trp	Hydrophobic substitution required. Enhances initial AZT resistance due to Lys70→Arg. Two-base mutation
Lys219→Gln/ Lys219→Glu	AZT	Affect interactions of residue 219 with residue 67 across the cleft, as well as formation of the 3′ pocket	Associated with mutations at positions 67, 70 and 215

mc, main chain; MDR, multidrug resistance (mutants resistant to AZT, ddI and ddC)

Asp67 and Lys 70, which have been implicated in RT resistance to NRTIs [42,43].

The Met184→Ile, Met184→Val or Met184→Thr [44–46] mutations might cause NRTI resistance through multiple structural changes. The structure of Met184→Ile HIV-1 RT in complex with DNA shows a repositioning of the template–primer along with smaller changes at the dNTP-binding site [47]. Modeling the β-L-enantiomer of 3TC (another NRTI) at the active sites of the Met184→Ile [47] and wild-type [10] enzymes suggests that resistance to 3TC might be due primarily to steric hindrance between the β-branched sidechains of Met184 mutant residues (isoleucine, threonine or valine) and the β-L-nucleoside ring of 3TC. The steric interaction in the Met184→Ile–DNA–3TC-triphosphate complex would be exacerbated by the positioning of the template–primer in the Met184→Ile–RT–DNA complex [47], consistent with the unusually high resistance reported for mutations at position 184 (>100 times the resistance due to any other single NRTI mutation [45,48,49]).

In AZT-resistant mutants, two base changes are required to convert position 215 to a hydrophobic residue (tyrosine or phenylalanine). This change could indirectly affect the conformation of the portion of the 3′ pocket that accommodates the azido group of AZT (Table 3, Figure 3). Mutation at a neighboring amino acid (e.g. position 210) could stabilize the Thr215→Tyr or Thr215→Phe mutants [50] and the Met41→Leu mutation might rearrange part of the wall of the 3′ pocket (Phe116), further altering the interactions between the azido group and the 3′ pocket (Table 3). Other residues associated with AZT resistance could either directly alter the interaction of RT with the dNTP triphosphate moiety (Lys70→Arg [10]) or indirectly affect the formation of the 3′ pocket through changes in interactions of fingers and palm [10]. Analysis of AZT resistance has been hampered by the difficulties of measuring a strong effect of

Figure 5

Structural interpretation of the mechanism of DNA polymerization by HIV-1 RT. **(a)**, **(b)** and **(c)** represent the structure of RT in the unliganded [2,3], binary complex [4], and ternary complex [10], respectively. Comparing (a) with (b) shows a large movement of the p66 thumb subdomain associated with DNA binding. Comparing (b) with (c) shows conformational changes in the fingers subdomain associated with dNTP binding. Commonly observed NRTI-resistance-mutation sites are shown as gold spheres.

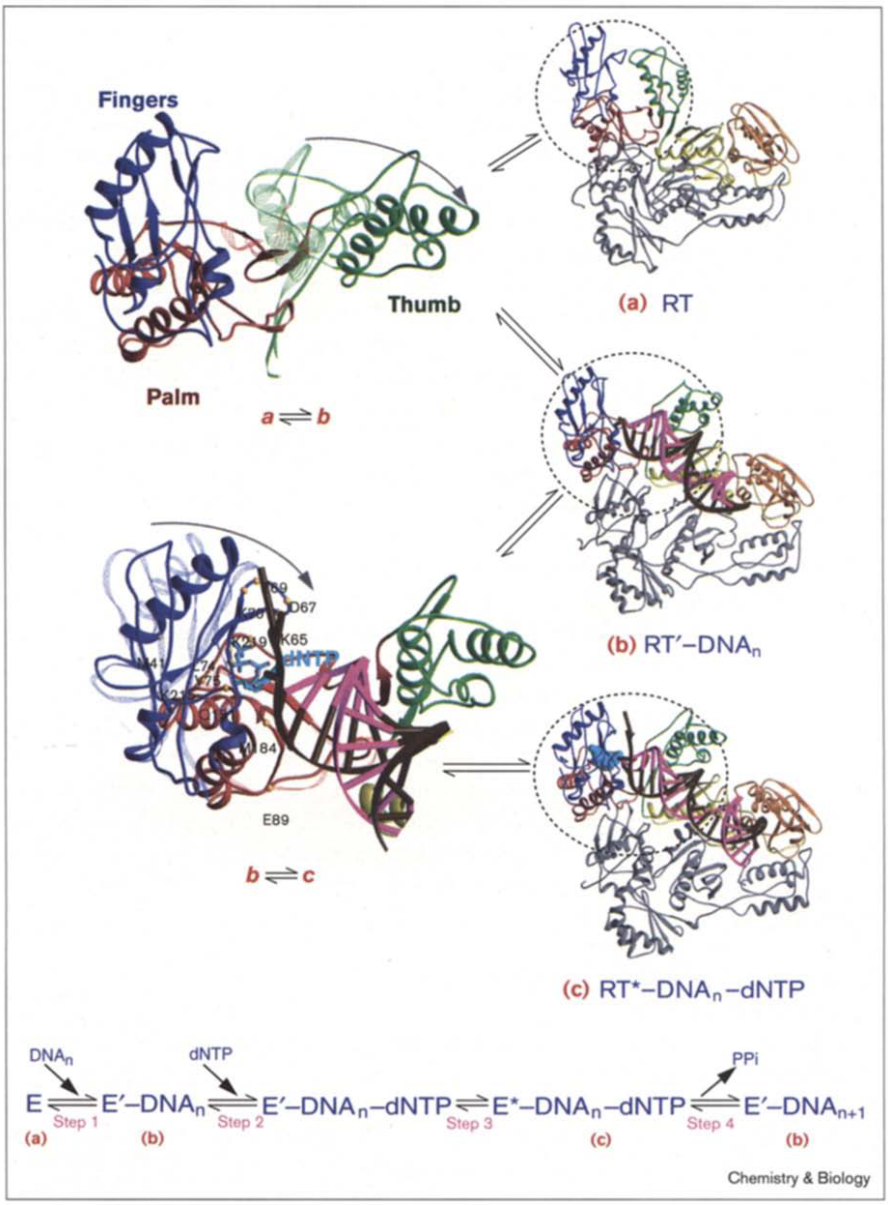

the resistance mutations on inhibition of HIV-1 RT by AZT triphosphate *in vitro*, however [51–54]. It has been suggested that resistance to AZT might result from hydrolytic removal of the AZT monophosphate of an AZT-monophosphate-terminated template–primer. This reaction occurs in the presence of millimolar concentrations of PP_i or dNTP and is more pronounced in RTs containing AZT-resistance mutations [55–57].

Finally, based on the RT–DNA–dNTP structure [10] we can now propose a model to explain why wild-type HIV-1 RT becomes sensitive to ddNTP inhibitors only when the template overhang is at least three nucleotides long [17]. It seems likely that there are hydrophobic interactions of the n+1, n+2 and n+3 template bases with conserved hydrophobic residues at positions 74, 61 and 24, respectively. These interactions could help to stabilize the β3–β4 strands in a conformation (Figure 4) that might permit favorable interactions of the incoming nucleotide with residues from/near β3–β4 (for example residues 65, 74, 75, 69/151) that have been implicated in resistance to ddNTP inhibitors. It is possible that in ddNTP binding these interactions can partly compensate for the loss of affinity that normally involves the 3′-OH of dNTPs.

Structures of intermediate steps in DNA polymerization

A general mechanism for nucleotide incorporation by the HIV-1 RT has been established and the rates for each of

the steps in the process have been determined (Figure 5) [58–63]. Polymerization begins with the binding of a template–primer to the unliganded enzyme (E) to form the E′–DNA_n complex (step 1). Nucleotide incorporation into the E′–DNA_n complex is initiated with binding of a dNTP to E′–DNA_n to form the E′–DNA_n–dNTP complex (step 2). The third step, which is the rate-limiting step in the reaction cycle, involves the conversion of E′–DNA_n–dNTP to an activated complex (E*–DNA_n–dNTP) [61,64,65]. The cycle is completed by an SN_2 nucleophilic attack by the 3′-OH primer terminus on the α-phosphate of dNTP that results in phosphodiester-bond formation and removal of the pyrophosphate product (step 4). After incorporation of the nucleotide, the polymerase can either dissociate from the template–primer and restart the cycle at another 3′-OH primer terminus (distributive mode of polymerization) or translocate along the elongated DNA product ('DNA_{n+1}') towards the new 3′-primer terminus (processive mode of polymerization). During the distributive mode of polymerization the cycle will restart from step 1; in the processive mode of polymerization the E′–DNA_{n+1} complex will continue the reaction from step 2. The unliganded RT with the thumb subdomain in the 'closed' position probably corresponds to the E form [2,3]. The structure of RT–DNA [12] is likely to represent an 'open state' of the enzyme that would occur after initial DNA binding (E′–DNA_n). A 'missing' structure in terms of an HIV-1 RT reaction scheme is the one that corresponds to the initial binding of dNTP, prior to the conformational change (E′–DNA–dNTP). At the time this review was being written, Li *et al.* [9] had just published the structure of ternary complex of Klentaq (E′–DNA–dNTP) with the fingers in the 'open' form. The structure of Huang *et al.* [10] is likely to represent the activated E*–DNA–dNTP 'closed' complex at the stage just after the rate-limiting step, in which the 3′-OH is poised to attack the α-phosphorus in an SN_2 nucleophilic reaction (with pyrophosphate as the leaving group). Finally, after addition of the dNTP is complete, and the complex has translocated to the next position, the fingers are likely to return to the 'open' conformation to allow binding of the next dNTP, thereby assuming a conformation (E′–DNA_{n+1}) likely to be the same as in the RT–DNA binary complex (E′–DNA_n) [12] (Figure 5).

Solution of the ternary structures of DNA polymerases has offered new insight into the fidelity of polymerization. Fidelity can be viewed as the ability to discriminate against incoming mismatched nucleotides, and to abort polymerization on template–primers already containing a mismatch. Discrimination against mismatched nucleotides can be accomplished at three levels: initial dNTP binding in the 'open' form, ensuing conformational changes to transform to the 'closed' form and catalytic incorporation. The structure of the ternary complex shows a 'tightly packed' dNTP-binding site that can carefully test the base-pair size and shape in the closed ternary state. Therefore, the rate-limiting conformational change can only be achieved for correct incoming nucleotides [66] that comply with the strict steric requirements [67]. Template–primers already containing a mismatch are likely to have a high dissociation constant due to unfavorable steric interactions of RT residues with mismatched base pairs that have incorrect geometry in the minor groove [10–12].

Conclusions and future perspectives

In conclusion, the structure of the HIV-1 RT–DNA–dNTP complex from the Harrison and Verdine laboratories [10] has provided valuable insights into how changes in the intricate interactions between the RT, dNTPs and the template–primer can affect resistance of HIV-1 RT to NRTIs. Furthermore, details of the specific interactions and structural changes at the dNTP-binding pocket should be valuable for designing new NRTIs. Comparisons with structures of unliganded and binary complexes of RT and with equivalent structures of other polymerases highlight the structural changes that occur during the course of DNA polymerization for all the polymerases whose structures are known.

Although this work has greatly extended our understanding of HIV-1 RT, further structural studies of inhibitor-bound wild-type and drug-resistant mutant HIV-1 RT structures promise to shed additional light on mysteries of fundamental scientific and medical importance.

References

1. Esnouf, R., Ren, J., Ross, R., Jones, Y., Stammers, D. & Stuart, D. (1995). Mechanism of inhibition of HIV-1 reverse transcriptase by non-nucleoside inhibitors. *Nat. Struct. Biol.* **2**, 303-308.
2. Rodgers, D.W., *et al.*, & Harrison, S.C. (1995). The structure of unliganded reverse transcriptase from the human immunodeficiency virus type 1. *Proc. Natl Acad. Sci. USA* **92**, 1222-1226.
3. Hsiou, Y., Ding, J., Das, K., Clark, A.D., Jr., Hughes, S.H. & Arnold, E. (1996). Structure of unliganded HIV-1 reverse transcriptase at 2.7 Å resolution: implications of conformational changes for polymerization and inhibition mechanisms. *Structure* **4**, 853-860.
4. Jacobo-Molina, A., *et al.*, & Arnold, E. (1993). Crystal structure of human immunodeficiency virus type 1 reverse transcriptase complexed with double-stranded DNA at 3.0 Å resolution shows bent DNA. *Proc. Natl Acad. Sci. USA* **90**, 6320-6324.
5. Ding, J., *et al.*, & Arnold, E. (1997). A review of HIV-1 RT structural studies and implications for drug design. In *Structure Based Drug Design*. (P. Veerapandian, ed), pp. 41-82, Marcel Dekker, Inc., New York.
6. Sawaya, M.R., Prasad, R., Wilson, S., Kraut, J. & Pelletier, H. (1997). Crystal structures of human DNA polymerase β complexed with gapped and nicked DNA: evidence for induced fit mechanism. *Biochemistry* **36**, 11205-11215.
7. Pelletier, H., Sawaya, M.R., Kumar, A., Wilson, S.H. & Kraut, J. (1994). Structures of ternary complexes of rat DNA polymerase β, a DNA template-primer, and ddCTP. *Science* **264**, 1891-1903.
8. Doublie, S., Tabor, S., Long, A.M., Richardson, C.C. & Ellenberger, T. (1998). Crystal structure of a bacteriophage T7 DNA replication complex at 2.2 Å resolution. *Nature* **391**, 251-258.
9. Li, Y., Korolev, S. & Waksman, G. (1998). Crystal structures of open and closed forms of binary and ternary complexes of the large fragment of *Thermus aquaticus* DNA polymerase: structural basis for nucleotide incorporation. *EMBO J.* **17**, 7514-7525.
10. Huang, H., Chopra, R., Verdine, G.L. & Harrison, S.C. (1998). Structure of a covalently trapped catalytic complex of HIV-1 reverse transcriptase: implications for drug resistance. *Science* **282**, 1669-1675.
11. Bebenek, K., *et al.*, & Kunkel, T.A. (1997). A minor groove binding track in reverse transcriptase. *Nat. Struct. Biol.* **4**, 194-197.

12. Ding, J., *et al.*, & Arnold, E. (1998). Structure and functional implications of the polymerase active site region in a complex of HIV-1 RT with double-stranded DNA and an antibody Fab fragment at 2.8 Å resolution. *J. Mol. Biol.* **284**, 1095-1111.
13. Eom, S.H., Wang, J. & Steitz, T.A. (1996). Structure of Taq polymerase with DNA at the polymerase active site. *Nature* **382**, 278-281.
14. Pelletier, H., Sawaya, M.R., Wolfle, W., Wilson, S.H. & Kraut, J. (1996). Crystal structures of human DNA polymerase β complexed with DNA: implications for catalytic mechanism, processivity and fidelity. *Biochemistry* **35**, 12742-12761.
15. Ding, J., Hughes, S.H. & Arnold, E. (1997). Protein–nucleic acid interactions and DNA conformation in a complex of human immunodeficiency virus type 1 reverse transcriptase with a double-stranded DNA template–primer. *Biopolymers* **44**, 125-138.
16. Kiefer, J.R., Mao, C., Braman, J.C. & Beese, L.S. (1998). Visualizing DNA replication in a catalytically active *Bacillus* DNA polymerase crystal. *Nature* **391**, 304-307.
17. Boyer, P.L., *et al.*, & Hughes, S.H. (1994). The sensitivity of wild-type human immunodeficiency virus type 1 reverse transcriptase to dideoxynucleotides depends on template length; the sensitivity of drug-resistant mutants does not. *Proc. Natl Acad. Sci. USA* **91**, 4882-4886.
18. Beese, L.S., Derbyshire, V. & Steitz, T.A. (1993). Structure of DNA polymerase I Klenow fragment bound to duplex DNA. *Science* **260**, 352-355.
19. Sarafianos, S.G., Pandey, V.N., Kaushik, N. & Modak, M.J. (1995). Site-directed mutagenesis of Arg72 of HIV-1 reverse transcriptase. *J. Biol. Chem.* **270**, 19279-19735.
20. Harris, D., Kaushik, N., Pandey, P.K., Yadav, P.N.S. & Pandey, V.N. (1998). Functional analysis of amino acid residues constituting the dNTP binding pocket of HIV-1 reverse transcriptase. *J. Biol. Chem.* **273**, 33624-33634.
21. Kaushik, N., Pandey, V.N. & Modak, M.J. (1996). Significance of O helix residues of *E. coli* pol I in DNA synthesis: Dynamics of dNTP binding pocket. *Biochemistry* **35**, 7256-7266.
22. Beese, L.S. & Steitz, T.A. (1991). Structural basis for the 3′-5′ exonuclease activity of *Escherichia coli* DNA polymerase I: a two-metal-ion mechanism. *EMBO J.* **10**, 25-33.
23. Huang, S.L. & Tsai, M.D. (1982). Does the Mg (II) ion interact with the alpha phosphate of adenosine triphosphate? An investigation by oxygen-17 nuclear magnetic resonance. *Biochemistry* **21**, 951-959.
24. Glonek, T. (1992). ^{31}P NMR of Mg-ATP in dilute solutions, complexation and exchange. *Int. J. Biochem.* **24**, 1533-1559.
25. Joyce, C.M. & Steitz, T.A. (1994). Function and structure relationships in DNA polymerases. *Ann. Rev. Biochem.* **63**, 777-822.
26. Patel, P.H., *et al.*, & Arnold, E. (1995). Insights into DNA polymerization mechanisms from structure and function analysis of HIV-1 reverse transcriptase. *Biochemistry* **34**, 5351-5363.
27. Larder, B.A., Purifoy, D.J.M., Powell, K.L. & Darby, G. (1987). Site-specific mutagenesis of AIDS virus reverse transcriptase. *Nature* **327**, 716-717.
28. Boyer, P.L., Ferris, A.L. & Hughes, S.H. (1992). Mutational analysis of the fingers domain of human immunodeficiency virus type-1 reverse transcriptase. *J. Virol.* **66**, 7533-7537.
29. Kaushik, N., Rege, N., Yadav, P.N., Sarafianos, S.G. & Modak, M.J. (1996). Biochemical analysis of catalytically crucial aspartate mutants of human immunodeficiency virus type 1 reverse transcriptase. *Biochemistry* **35**, 11536-11546.
30. Tabor, S. & Richardson, C.C. (1995). A single residue in DNA polymerases of the *Escherichia coli* DNA polymerase I family is critical for distinguishing between deoxy- and dideoxyribonucleotides. *Proc. Natl Acad. Sci. USA* **92**, 6339-6343.
31. Tesmer, J.G., Sunahara, R.K., Gilman, A.G. & Sprang, S.R. (1997). Crystal structure of the catalytic domains of adenylyl cyclase in a complex with Gsα-GTPγS. *Science* **278**, 1907-1916.
32. Tesmer, J.G., & Sprang, S.R. (1998). The structure, catalytic mechanism and regulation of adenylyl cyclase. *Curr. Opin. Struct. Biol.* **8**, 713-719.
33. Shirasaka, T., *et al.*, & Mitsuya, H. (1995). Emergence of human immunodeficiency virus type 1 variants with resistance to multiple dideoxynucleosides in patients receiving therapy with dideoxynucleosides. *Proc. Natl. Acad. Sci. USA* **92**, 2398-2402.
34. Iversen, A.K.N., *et al.*, & Merigan, T.C. (1996). Multidrug-resistant HIV1 strains resulting from combination antiretroviral therapies. *J. Virol.* **70**, 1086-1090.
35. Sarafianos, S.G., Pandey, V.N., Kaushik, N. & Modak, M.J. (1995). Glutamine 151 participates in the substrate dNTP binding function of HIV-1 reverse transcriptase. *Biochemistry* **34**, 7207-7216.
36. St. Clair, M.H., *et al.* & Larder, B.A. (1991). Resistance to ddI and sensitivity to AZT induced by a mutation in HIV-1 reverse transcriptase. *Science* **253**, 1557-1559.
37. Gu, Z., *et al.*, & Wainberg, M.A. (1994). Identification of a mutation at codon 65 in the IKKK motif of reverse transcriptase that encodes human immunodeficiency virus resistance to 2′,3′-dideoxycytidine and 2′,3′-dideoxy-3′-thiacytidine. *Antimicrob. Agents Chemother.* **38**, 275-281.
38. Zhang, D., *et al.*, & D' Aquila, R.T. (1994). Resistance to 2′,3′-dideoxycytidine conferred by a mutation in codon 65 of the HIV-1 reverse transcriptase. *Antimicrob. Agents Chemother.* **38**, 282-287.
39. Gu, Z., *et al.*, & Wainberg, M.A. (1995). K65R mutation of human immunodeficiency virus type 1 reverse transcriptase encodes cross-resistance to 9-(2-phosphonylmethoxyethyl)adenine. *Antimicrob. Agents. Chemother.* **39**, 1888-1891.
40. Winters, M.A., *et al.*, & Merigan, T.C. (1998). A 6-basepair insert in the reverse transcriptase of HIV-1 confers resistance to multiple nucleoside inhibitors. *J. Clin. Invest.* **102**, 1769-1775.
41. Larder, B.A. & Stammers, D.K. (1999). Closing in on HIV drug resistance. *Nat. Struct. Biol.* **6**, 103-106.
42. Larder, B.A. & Kemp, S.D. (1989). Multiple mutations in HIV-1 reverse transcriptase confer high-level resistance to zidovudine (AZT). *Science* **246**, 1155-1158.
43. Larder, B.A., Coates, K.E. & Kemp, S.D. (1991). Zidovudine-resistant human immunodeficiency virus selected by passage in cell culture. *J. Virol.* **65**, 5232-5236.
44. Gao, Q., *et al.*, & Wainberg, M.A. (1993). The same mutation that encodes low-level human immunodeficiency virus type-1 resistance to 2′,3′-dideoxyinosine and 2′,3′-dideoxycytidine confers high-level resistance to the (-) enantiomer of 2′,3′-dideoxy-3′-thiacytidine. *Antimicrob. Agents Chemother.* **37**, 1390-1392.
45. Tisdale, M., Kemp, S.D., Parry, N.R. & Larder, B.A. (1993). Rapid *in vitro* selection of human immunodeficiency virus type 1 resistant to 3′-thiacytidine inhibitors due to a mutation in the YMDD region of reverse transcriptase. *Proc. Natl Acad. Sci. USA* **90**, 5653-5656.
46. Keulen, W., Back, N.K.T., Van Wijk, A., Boucher, C.A.B. & Berkhout, B. (1997). Initial appearance of the 184Ile variant of Lamivudine-treated patients is caused by the mutational bias of human immunodeficiency virus type 1 reverse transcriptase. *J. Virol.* **71**, 3346-3350.
47. Sarafianos, S.G., *et al.*, & Arnold, E. (1998). Structures of Met184→Ile and Met184→Val mutants of HIV-1 reverse transcriptase with and without bound nucleic acid reveal template-primer repositioning and steric hindrance mechanism for lamivudine resistance. *Antiviral Therapy* **3,** Supplement 117-18.
48. Schinazi, R.F., *et al.*, & Mellors, J.W. (1993). Characterization of human immunodeficiency virus resistant to oxathiolane-cytosine nucleosides. *Antimicrob. Agents Chemother.* **37**, 875-881.
49. Gosselin, G., *et al.*, & Imbach, J.L. (1994). Anti-human immunodeficiency virus activities of the beta-L-enantiomer of 2′,3′-dideoxycytidine and its 5-fluoro derivative *in vitro*. *Antimicrob. Agents Chemother.* **38**, 1292-1297.
50. Hooker, D.J., *et al.*, & Deacon, N.J. (1996). An *in vivo* mutation from leucine to tryptophan at position 210 in HIV-1 reverse transcriptase contributes to high-level resistance to AZT. *J. Virol.* **70**, 8010-8018.
51. Lacey, S.F., *et al.*, & Larder, B.A. (1992). Biochemical studies on the reverse transcriptase and RNase H activities from human immunodeficiency virus strains resistant to 3′-azido-3′-deoxythymidine. *J. Biol. Chem.* **267**, 15789-15794.
52. Larder, B.A. (1992). AZT resistance suppressed by a mutation conferring HIV-1 resistance to non-nucleoside reverse transcriptase inhibitors. *Antimicrob. Agents Chemother.* **36**, 1171-1174.
53. Kimberlin, D.W., *et al.*, & Whitley, R.J. (1995). Molecular mechanisms of antiviral resistance. *Antiviral Res.* **26**, 369-401.
54. Krebs, R., Immendorfer, U., Thrall, S.H., Wohrl, B.M. & Goody, R.S. (1997). Single-Step kinetics of HIV-1 reverse transcriptase mutants responsible for virus resistance to nucleoside inhibitors zidovudine and 3TC. *Biochemistry* **36**, 10292-10300.
55. Arion, D., Borkow, G., Gu, Z., M., W. & Parniak, M.A. (1998). Phenotypic mechanism of HIV-1 resistance to AZT: Increased polymerization processivity and enhanced sensitivity to pyrophosphate of the mutant viral reverse transcriptase. *Biochemistry* **37**, 15908-15917.
56. Canard, B., Sarfati, S.R. & Richardson, C.C. (1998). Enhanced binding of AZT-resistant HIV-1 RT to the AZT-5′-monophosphate-terminated primer. *J. Biol. Chem.* **273**, 14596-14604.
57. Meyer, P.R., Matsuura, S.E., So, A.G. & Scott, W.A. (1998). Unblocking of chain-terminated primer by HIV-1 reverse transcriptase through a nucleotide-dependent mechanism. *Proc. Natl Acad. Sci. USA* **95**, 13471-13476.

58. Kuchta, R.D., Mizrahi, V., Benkovic, P.A., Johnson, K.A. & Benkovic, S.J. (1987). Kinetic mechanism of DNA polymerase I (Klenow). *Biochemistry* **26**, 8410-8417.
59. Majumdar, C., Abbotts, J., Broder, S. & Wilson, S.H. (1988). Studies on the mechanism of human immunodeficiency virus reverse transcriptase: steady-state kinetics, processivity and polynucleotide inhibition. *J. Biol. Chem.* **263**, 15657-15665.
60. Dahlberg, M.E. & Benkovic, S.J. (1991). Kinetic mechanism of DNA polymerase I (Klenow fragment): identification of a second conformational change. *Biochemistry* **30**, 4835-4843.
61. Kati, W.M., Johnson, K.A., Jerva, L.F. & Anderson, K.S. (1992). Mechanism and fidelity of HIV reverse transcriptase. *J. Biol. Chem.* **267**, 25988-25997.
62. Reardon, J.E. (1993). Human immunodeficiency virus reverse transcriptase. *J. Biol. Chem.* **268**, 8743-8751.
63. Hsieh, J., Zinnen, S. & Modrich, P. (1993). Kinetic mechanism of the DNA-dependent DNA polymerase activity of human immunodeficiency virus reverse transcriptase. *J. Biol. Chem.* **268**, 24607-24613.
64. Rittinger, K., Divita, G. & Goody, R. (1995). Human immunodeficiency virus reverse transcriptase substrate-induced conformational changes and the mechanism of inhibition by nonnucleoside inhibitors. *Proc. Natl Acad. Sci. USA* **92**, 8046-8049.
65. Spence, R.A., Kati, W.M., Anderson, K.S. & Johnson, K.A. (1995). Mechanism of inhibition of HIV-1 reverse transcriptase by nonnucleoside inhibitors. *Science* **267**, 988-993.
66. Johnson, K.A. (1993). Conformational coupling in polymerase fidelity. *Annu. Rev. Biochem.* **62**, 685-713.
67. Moran, S., Ren, X.F.R., Rumney, S.I. & Kool, E.T. (1997). Difluorotoluene, a nonpolar isostere of thymine, codes specifically and efficiently for adenine in DNA replication. *J. Am. Chem. Soc.* **119**, 2056-2057
68. De Jong J.J., *et al.*, & Jurriaans, S. (1999). Insertion of two amino acids combined with changes in reverse transcriptase containing tyrosine-215 of HIV-1 are resistant to multiple nucleoside analogs. *AIDS* **13**, 75-80.